Radical Cation Spectroscopy of Substituted Alkyl Phenyl Ketones via Tunnel Ionization

ARTICLE *in* CHEMICAL PHYSICS · OCTOBER 2014

Impact Factor: 1.65 · DOI: 10.1016/j.chemphys.2014.05.019

Chemical Physics 442 (2014) 81–85

Contents lists available at ScienceDirect

Chemical Physics

journal homepage: www.elsevier.com/locate/chemphys

Radical cation spectroscopy of substituted alkyl phenyl ketones via tunnel ionization

Timothy Bohinski [a,b], Katharine Moore Tibbetts [a,b], Kristin Munkerup [d], Maryam Tarazkar [a,b], Dmitri A. Romanov [a,c], Spiridoula Matsika [b], Robert J. Levis [a,b,*]

[a] Center for Advanced Photonics Research, Temple University, Philadelphia, PA 19122, United States
[b] Department of Chemistry, Temple University, Philadelphia, PA 19122, United States
[c] Department of Physics, Temple University, Philadelphia, PA 19122, United States
[d] Department of Chemistry, University of Copenhagen, Universitetsparken 5, DK-2100 Copenhagen Ø, Denmark

ARTICLE INFO

Article history:
Available online 2 June 2014

Keywords:
Radical cation
Tunnel ionization
Electronic spectroscopy
Dihedral angle

ABSTRACT

Mass spectra are measured for 2′-, 3′- and 4′-(*ortho*, *meta* and *para*) methyl substituted alkyl phenyl ketones excited at wavelengths ranging from 1200 to 1500 nm in the strong field regime. The selective loss of a methyl group from the acetyl group of the parent molecular ion upon excitation at ~1370 nm is attributed to an electronic resonance between ground D_0 and excited D_2 state of the radical cation. Depletion of the parent molecular ion is enhanced as the methyl substituent is moved from the 2′ to 3′ to 4′ position on the phenyl ring with respect to the acetyl group. The phenyl-acetyl dihedral angle is the relevant coordinate enabling excitation to the dissociative D_2 state. Calculations on the radical cation of 2′-methylacetophenone show two stable geometries with dihedral angles of 7 degrees and 63 degrees between the phenyl and acetyl groups. The barrier to rotation for the 2′ isomer limits population transfer to the D_2 state. In contrast, calculations on the radical cations of 3′- and 4′-methylacetophenone reveal no rotational barrier to prevent population transfer to the excited state, which is consistent with the enhanced dissociation yield in comparison with the 2′ substitution. The enhanced dissociation of the 4′ isomer as compared to the 3′ isomer is attributed to its lower moment of inertia about the dihedral angle.

1. Introduction

An emerging theme in the area of controlling chemical reactions in the strong field regime is the role of radical cation excited states in the dynamics of molecular dissociation [1,2]. When a molecule interacts with a strong field laser pulse (>10^{13} W cm^{-2}), the radical cation can be produced via multiphoton and/or tunnel ionization [3–7], populating one or more electronic states. To distinguish tunnel from multiphoton ionization, the Keldysh parameter γ may be utilized [8,9]. This parameter is defined as the ratio of the laser frequency ω_o to a characteristic tunneling frequency ω_t

$$\gamma = \frac{\omega_o}{\omega_t} = \frac{\omega_o\sqrt{2\mathrm{IP}m_e}}{eE_o} \quad (1)$$

where IP is the ionization potential, E_0 is the laser field magnitude, m_e is the electron mass and e is the electron charge. If $\gamma \gg 1$, multiphoton ionization is the dominant mechanism, while tunnel ionization dominates if $\gamma \ll 1$, as illustrated in Fig. 1. Multiphoton ionization in the strong field regime typically populates a number of cation electronic states $|e_0\rangle$, $|e_1\rangle$, $|e_2\rangle$,... due to ladder climbing [10]. These states can relax through internal conversion to produce vibrationally hot molecules that can undergo a high degree of fragmentation. Although lowering the intensity of the excitation pulse that initiates multiphoton ionization can help minimize ladder climbing, this also decreases the observed ion signal. In the adiabatic limit, tunnel ionization leaves the molecule in its ground radical cation state $|e_0\rangle$ with little excess vibrational energy.

The contrast between molecular fragmentation patterns upon multiphoton and tunnel ionization was first demonstrated in linear polyenes [7], where excitation at 800 nm resulted in a high degree of fragmentation, while excitation at 1450 nm produced primarily singly and doubly charged parent molecular ion. The fragmentation at shorter wavelengths was explained in terms of non-adiabatic multi-electron dynamics. Reduced molecular fragmentation upon excitation with near-IR wavelengths as compared to 800 nm has since been observed in other molecules including naphthalene

* Corresponding author at: Center for Advanced Photonics Research, Temple University, Philadelphia, PA 19122, United States. Tel./fax: +1 215 204 5241x6179.
E-mail address: rjlevis@temple.edu (R.J. Levis).

http://dx.doi.org/10.1016/j.chemphys.2014.05.019
0301-0104/

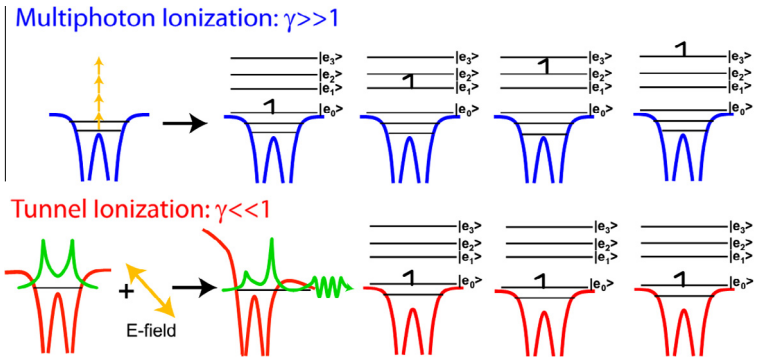

Fig. 1. A depiction of the distribution of electronic states in a molecule after multiphoton ionization (MPI) and tunnel ionization.

[11], anthracene [12], alkylphenols [13] and acetophenone [14]. We propose that the adiabatic ionization mechanism at longer wavelengths has important consequences for electronic spectroscopy and coherent control, as the "cold" parent molecular ion formed by tunnel ionization can be used as a "launch state" for further excitation [15].

Upon formation of a radical cation, excitation to higher lying electronic states can result in dissociation. Cationic resonances observed via photoelectron spectroscopy have been shown to correlate with strong field fragmentation patterns in $Ni(CO)_4^+$ and $Fe(CO)_5^+$, where enhanced fragmentation was observed upon excitation with the resonant wavelengths of 1350 nm for $Ni(CO)_4^+$ and 800 nm for $Fe(CO)_5^+$ [16]. Enhanced fragmentation of cycloketones upon excitation with 394 nm as compared to 788 nm was attributed to features in their respective radical cation photoabsorption spectra [17,18]. Similar dissociation was observed for large aromatic molecules excited with 1400 nm [12]. Mass-resolved, strong field excitation using laser pulses ranging from 1200 to 1500 nm has revealed the existence of a cationic resonance at 1370 nm in alkyl phenyl ketones. The resonance is supported by calculations of the cationic ground and excited state energies [1]. Calculations show the existence of radical cationic states and reveal their role in fragmentation mechanisms [1,19–22]. Transient cationic resonances have also been observed in pump–probe studies on halomethanes [23,24] and azobenzene [19].

We have recently reported that a cationic resonance in alkyl phenyl ketones upon excitation with ~0.9 eV (1370 nm) IR photons leads to selective formation of the benzoyl fragmentation product, supported by quantum calculations of the acetophenone and propiophenone radical cations [1]. Calculations show that the ground ionic surface D_0 and second ionic excited state D_2 are separated by 0.87 and 0.88 eV at the energetic minimum of the ground radical cation surface for acetophenone and propiophenone, respectively. The formation mechanism of the benzoyl fragment upon excitation from D_0 to D_2 is shown in Fig. 2. Upon vertical ionization, the radical cation of acetophenone is produced at a torsional angle of 0 degrees between the phenyl and acetyl moieties. Subsequent relaxation of the cation increases the phenyl-acetyl dihedral angle to 44 degrees, with the oscillator strength $f(D_0–D_2)$ between the two states increasing from zero upon vertical excitation to 0.046 at the relaxed geometry. Once the molecule reaches this geometry, the trailing edge of the laser pulse excites a resonant transition to the D_2 state. The wavepacket then propagates on the D_2 surface to a conical intersection of the D_0, D_1, and D_2 ionic surfaces at a torsional angle of zero degrees. The nonadiabatic nature of the conical intersection converts the electronic energy in the torsional coordinate to vibrational energy in the C—CH_3 bond length coordinate leading to bond dissociation.

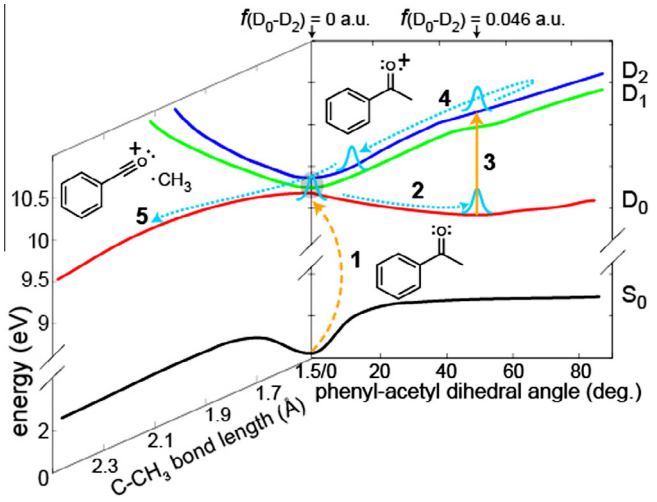

Fig. 2. The proposed mechanism for the dissociation of the acetophenone radical cation [1]. The black, red, green, and blue curves correspond to the S_0, D_0, D_1, and D_2 states respectively. Tunnel ionization (step 1) launches a torsional wavepacket on the ground state D_0 of the parent molecular ion, which relaxes to its equilibrium geometry (step 2). At the energy minimum, the wavepacket undergoes a one-photon resonant transition to the D_2 state (step 3). The wavepacket proceeds down the D_2 surface reaching a conical intersection (step 4) that converts electronic energy to vibrational energy leading to bond dissociation along the C—CH_3 bond coordinate (step 5). (For interpretation of the references to colour in this figure legend, the reader is referred to the web version of this article.)

This work investigates fragmentation yields in the family of methyl substituted alkyl phenyl ketones, 2′-, 3′-, and 4′-methylacetophenone. Mass spectra are measured as a function of strong field excitation wavelength ranging from 1200 to 1500 nm. Calculations are performed on the molecules to determine the nuclear configurations corresponding to the energy minima of the neutral molecules and radical cations. The results are rationalized in terms of the energies and phenyl-acetyl dihedral angles in the respective optimized geometries of the radical cations of 2′-, 3′-, and 4′-methylacetophenone.

2. Experimental

The apparatus used to perform the measurements of the electronic structure of a radical cation has been described previously [1]. Briefly, a Ti:Sapphire amplifier producing 1 mJ, 50 fs pulses was used to pump an optical parametric amplifier (OPA) to generate tunable IR pulses from 1150 to 1550 nm with pulse durations from 50 to 100 fs. Pulse durations for the following experiments were maintained at 60 fs across the tuning range as measured by

frequency-resolved optical gating. The excitation beam was focused by a plano-convex lens with $f = 20$ cm to reach intensities ranging between 2.0 and 8.0×10^{13} W cm^{-2} in the extraction region of a time-of flight mass spectrometer (TOF-MS) with a base pressure 1.3×10^{-6} Pa. Attenuation of the pulse energy was performed using a circular variable neutral density filter. Gas phase samples of 2′-, 3′-, and 4′-methylacetophenone (Sigma–Aldrich) were leaked into the vacuum chamber by a variable leak valve to attain a sample pressure of 4.6×10^{-4} Pa. Mass spectra were recorded as a function of both laser wavelength and intensity. The laser intensity at each wavelength was internally calibrated for each measurement by measuring the ion yield from xenon introduced using a second leak valve [25]. Electronic structure calculations were performed using the Gaussian 09 program package [26]. The geometries of the 2′-, 3′-, and 4′-methylacetophenone neutral molecules and radical cations were optimized at the B3LYP/6-311++G(d,p) level of theory.

3. Results/discussion

The upper panel of Fig. 3 shows the mass spectra of 2′-methylacetophenone ionized with 800 nm (top, red) and 1240 nm (bottom, blue) at a laser intensity of 5×10^{13} W cm^{-2}, with associated Keldysh parameters as indicated. The mass spectrum at 800 nm shows a higher yield of small fragment ions ($m/z < 91$), with the benzoyl ion (m/z 119) as the dominant peak. In contrast, at 1240 nm, the dominant peak is the parent ion (m/z 134) and a significantly reduced yield of small fragments is observed. These results can be understood by considering the respective ionization mechanisms at both wavelengths. The Keldysh parameter at 800 nm is 1.14, indicating a higher contribution from multiphoton ionization as compared to 1240 nm, where the lower Keldysh parameter of 0.73 results in a higher contribution from tunnel ionization. Recently, nonresonant strong field excitation at 800 nm of methyl-substituted acetophenone molecules has revealed fragmentation patterns characteristic of a multiphoton ionization mechanism [10]. The lower panel of Fig. 3 displays the fractional yield of small mass fragments ($m/z \leqslant 91$) as a function of laser intensity at various wavelengths and the fractional yield of the small mass fragments is similar (small probability and featureless spectrum) for all three isomers. At all infrared wavelengths, the yield of small mass fragments is much less than at 800 nm. The low degree of fragmentation and the corresponding abundance of the parent ion suggest that the ground ionic state is formed upon ionization at these wavelengths.

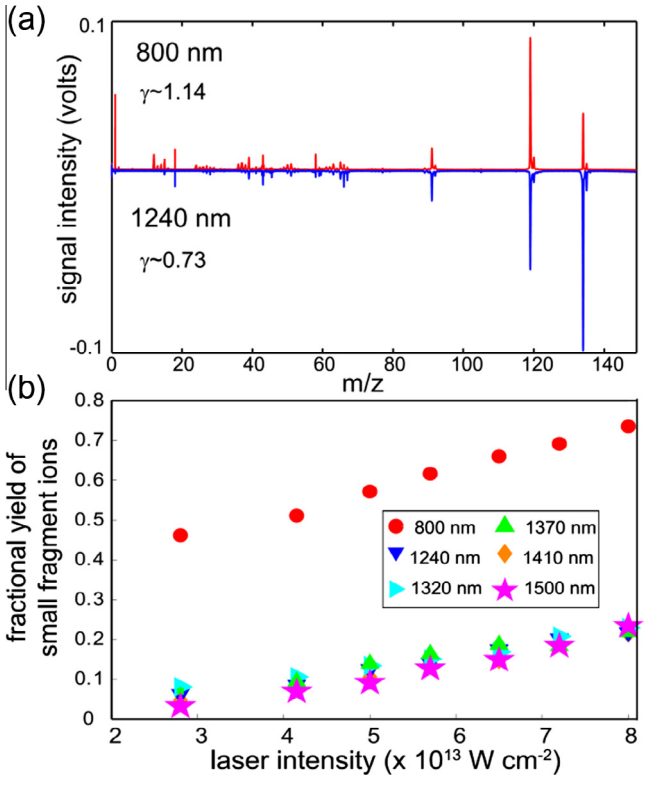

Fig. 3. (a) Mass spectra of 2-methylacetophenone at 800 nm (red) and 1240 nm (blue, inverted) with their respective Keldysh parameters. The laser intensity is 5×10^{13} W cm^{-2}. (b) The yield of small fragments ions, $m/z < 91$, as a function of laser intensity as a function of excitation wavelength. (For interpretation of the references to colour in this figure legend, the reader is referred to the web version of this article.)

The yields of the benzoyl and parent ions (normalized to the maximum observed benzoyl ion yield) as a function of excitation wavelength are plotted for 2′-, 3′- and 4′-methylacetophenone in Fig. 4 at a laser intensity of $\sim 5 \times 10^{13}$ W cm^{-2}. The ion yields are not sensitive to the excitation wavelength for wavelengths shorter than 1300 nm, with the parent molecular ion dominating the mass spectrum. At wavelengths longer than 1300 nm, the benzoyl ion yield increases and the parent ion yield decreases until the maximum benzoyl and minimum parent ion yields are observed at ~1370 nm. As the excitation wavelength is increased further, the benzoyl and parent ions return to a yield similar to that measured at wavelengths shorter than 1300 nm. Based on prior measurements and calculations of the molecules acetophenone and propiophenone [1], the frequency dependent fragmentation suggests the presence of a resonance between the ground cationic state and a dissociative cationic state leading to selective formation of the benzoyl fragment ion. The resonance in acetophenone and propiophenone was also centered around 1370 nm, suggesting that methyl substitution on the phenyl ring does not affect the energy spacing of the low-lying cationic states.

Inspection of Fig. 4 shows that the depletion of the parent molecular ion at 1370 nm is more pronounced as the methyl group position changes from *ortho* to *meta* to *para* with respect to the acetyl group. This result can be rationalized by taking into account the torsional dynamics of the radical cation following ionization. As illustrated in Fig. 2, the radical cation is formed at the neutral geometry with a zero degree dihedral angle between the phenyl and acetyl groups. At this angle the oscillator strength for the transition coupling from the ground to the low lying excited states is identically zero due to symmetry restrictions [1]. In the case of acetophenone, the minimum energy on the D_0 surface is reached at a dihedral angle of 44 degrees, so the initial ionization event results in the launching of a wavepacket along the torsional coordinate towards the energy minimum [14]. As the acetyl group rotates out of plane, the oscillator strength between the ground state D_0 and the excited state D_2 becomes nonzero, which allows D_2 to be populated via a one-photon transition. This excitation occurs on the trailing edge of the excitation pulse at the optimal geometry. Excitation to the D_2 state ultimately results in passage through a conical intersection, leading to depletion of the parent ion and enhanced formation of benzoyl product [1], as illustrated in Fig. 2. A time-resolved wavepacket dynamics calculation reveals that the torsional period is approximately 650 fs and the optimal radical cation geometry of 44 degrees is reached in ~200 fs [15]. This timescale allows a photon from the lower intensity trailing edge of the pulse to excite the wavepacket entering the bright region.

The trend in parent ion depletion as a function of methyl substitution position is explained in terms of the calculated neutral and optimized geometries and energies of the ground state radical cations, which are presented in Table 1.

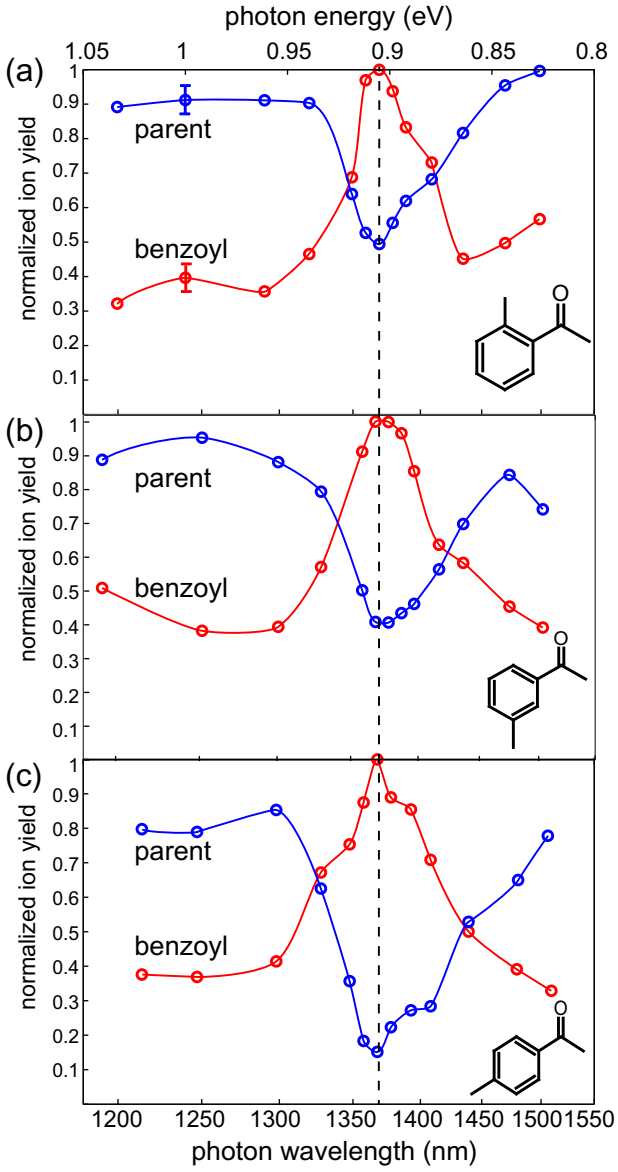

Fig. 4. The mass spectral response of the benzoyl and parent ions as a function of excitation wavelength for (a) 2′-, (b) 3′- and (c) 4′-methylacetophenone. Each plot is normalized to the benzoyl ion at 1370 nm. The vertical dashed line shows the position of the ionic resonance centered at 1370 nm. The laser intensity for all scans was 5×10^{13} W cm^{-2}. The error bars in (a) are shown for the parent and benzoyl ion yield at 1240 nm and are consistent with the error for other data points throughout Fig. 4.

The reduced parent ion depletion in 2′-methylacetophenone can be attributed to its radical cation having two ground state geometries corresponding to energy minima, labeled (a) and (b) in Table 1. The calculations reveal two stable radical cation geometries where (a), a local minimum, has a torsional angle of 7 degrees and (b), the global minimum, has a torsional angle of 63 degrees as shown in Fig. 5. For comparison, the neutral geometry is shown in Fig. 5(c). Fig. 5(a) shows that the locally optimal geometry (a) arises from a favorable interaction between a hydrogen atom from the *ortho* methyl group and the carbonyl oxygen, as indicated by the dotted blue line. This interaction arises in geometry (a), where the distance between the methyl hydrogen and carbonyl oxygen is only 2.1 Å, while the longer distances in (b) and (c) suggest that the strength of the interaction is negligible at these geometries. The presence of two stable geometries indicates the existence of a barrier to rotation between the phenyl and acetyl groups, which inhibits motion along the torsional coordinate. This slowing of the torsional wavepacket motion following ionization suppresses excitation to the D_2 state because the molecule is less likely to reach the geometry with a large transition dipole moment that promotes the one-photon excitation within the duration of the excitation pulse.

Slower motion of the torsional wavepacket in 2′-methylacetophenone as compared to the 3′ and 4′ isomers is also expected based on the difference between the energy of the vertical geometry and the optimized geometry of the radical cation ($E_{\text{neut-opt}}$). $E_{\text{neut-opt}}$ increases as the position of the methyl changes from *ortho* to *meta* to *para*. The larger values of $E_{\text{neut-opt}}$ for 3′- and 4′-methylacetophenone are similar to that of acetophenone [15], suggesting that the torsional wavepacket in these isomers gains kinetic energy more quickly than 2′, allowing these molecules to access the bright geometry within the excitation pulse duration. In contrast, the energy gap in 2′-methylacetophenone is about 0.1 eV smaller which makes the wavepacket traverse more slowly in the torsional coordinate so that it is less likely to reach the bright geometry within the duration of the excitation pulse. The amount of benzoyl production and parent depletion is also expected to depend on the oscillator strengths between D_0 and D_2. The oscillator strengths at the optimized geometries increase as the methyl substitution changes from *ortho* (7 degrees) to *meta* to *para*. The larger oscillator strengths for 3′- and 4′-methylacetophenone suggests a stronger coupling between D_0 and D_2, resulting in more parent ion depletion and contributing to the deeper lineshapes in Fig. 4. Finally, the enhanced depletion of the parent ion in 4′-methylacetophenone as compared to 3′-methylacetophenone can be explained in terms of its smaller moment of inertia, allowing the torsional wavepacket motion to proceed more quickly towards the critical geometry. In all three isomers, the axis of rotation is along the C(phenyl)-C(acetyl) bond. Thus, when the methyl group is in the 2′ or 3′ position, the moment of inertia is significantly larger because the methyl group is not on the rotational axis. The larger moment of inertia for the 2′ and 3′ isomers slows the rotation as compared to when the methyl group is in the 4′ position. Note that the moment of inertia for the 4′ isomer is nearly the same as that for acetophenone. The similar moment of inertia in 4′-methylacetophenone explains why its spectral response is

Table 1
Energies and angles of the radical cations of 2′-, 3′- and 4′-methyl-acetophenone: experimental vertical ionization potentials (IP_{exp}) [28], calculated values of vertical ionization potentials (IP_{calc}), the energy difference between the neutral geometry and the optimized geometry on the cationic ground state surface ($E_{\text{neut-opt}}$),the dihedral angle in the optimized radical cations, the M—CH_3 bond dissociation energies [27], and the calculated oscillator strengths for the D_0–D_2 transition. 2′-methyl-acetophenone has two minima on the cationic surface suggesting an energy barrier towards rotation of the acetyl group.

	2′-Methyl-acetophenone (a)	2′-Methyl-acetophenone (b)	3′-Methyl-acetophenone	4′-Methyl-acetophenone
IP_{exp} (eV)	9.15	9.15	9.14	9.12
IP_{calc} (eV)	8.88	8.88	8.91	8.91
$E_{\text{neut-opt}}$ (eV)	0.15	0.19	0.24	0.25
Phenyl-acetyl dihedral angle (°)	7	63	35	43
Bond dissociation energy (eV)	0.78		0.94	0.83
Oscillator strength	0.0009	0.0388	0.0247	0.0357

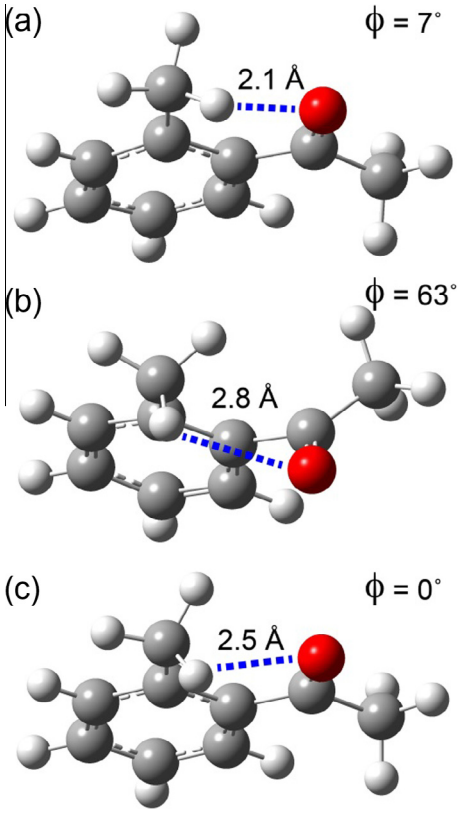

Fig. 5. Geometries of 2′-methylacetophenone, indicating distance between the methyl hydrogen and carbonyl oxygen by the blue dotted lines. (a) Local minimum in the radical cation with an interaction between methyl hydrogen and carbonyl oxygen. (b) Global minimum of the radical cation. (c) Neutral geometry. (For interpretation of the references to colour in this figure legend, the reader is referred to the web version of this article.)

practically identical to that of acetophenone when using a 60 fs pulse [14]. In contrast, the slower rotation of 3′-methylacetophenone decreases the fraction of the wavepacket accessing the bright region within the duration of the pulse, resulting in less depletion of the parent molecular ion.

4. Conclusion

The wavelength dependent mass spectral response of methyl-substituted acetophenone derivatives was found to be similar to that of acetophenone and propiophenone, indicating the presence of a resonance between the D_0 launch state and the dissociative D_2 state of the radical cation. The similarity of resonance position indicates that methyl substitution does not significantly alter the energies of the low-lying cationic states. The depletion of the parent molecular ion upon resonant excitation as a function of the position of the methyl substitution on the phenyl ring increases from *ortho* to *meta* to *para*. The trend can be explained by the effect of the substitution position on the motion of the torsional wavepacket. Calculations of the dihedral angles and ground state energies of the neutral and optimized geometries for each isomer reveal the presence of a favorable interaction between the methyl hydrogen and carbonyl oxygen in the *ortho* isomer that limits torsional motion which hinders access to the bright geometry. In addition, the *meta* isomer has a larger moment of inertia in comparison with the *para* isomer, slowing the torsional motion to the bright geometry. The measurements and calculations are useful for understanding the role that substitution on the phenyl ring plays in the strong field dissociation of radical cations of alkyl phenyl ketones. Future work will be aimed at understanding the effect of other substituent groups on the spectroscopy of radical cations.

Conflict of interest

The authors declare no competing financial interests.

Acknowledgement

We acknowledge the support of the National Science Foundation through Grant CHE0957694.

References

[1] T. Bohinski, K. Moore Tibbetts, M. Tarazkar, D. Romanov, S. Matsika, R. Levis, J. Phys. Chem. A 117 (2013) 12374.
[2] S.K. Lee, H.B. Schlegel, W. Li, J. Phys. Chem. A 117 (2013) 11202.
[3] M.J. DeWitt, R.J. Levis, Phys. Rev. Lett. 81 (1998) 5101.
[4] R.J. Levis, M.J. DeWitt, J. Phys. Chem. A 103 (1999) 6493.
[5] A.N. Markevitch, S.M. Smith, D.A. Romanov, H.B. Schlegel, M.Y. Ivanov, R.J. Levis, Phys. Rev. A 68 (2003) 4.
[6] S.M. Smith, X.S. Li, A.N. Markevitch, D.A. Romanov, R.J. Levis, H.B. Schlegel, J. Phys. Chem. A 109 (2005).
[7] M. Lezius, V. Blanchet, M.Y. Ivanov, A. Stolow, J. Chem. Phys. 117 (2002) 1575.
[8] L.V. Keldysh, Sov. Phys. JETP-USSR 20 (1965) 1307.
[9] M.J. DeWitt, R.J. Levis, J. Chem. Phys. 108 (1998) 7739.
[10] X. Zhu, V.V. Lozovoy, J.D. Shah, M. Dantus, J. Phys. Chem. A 115 (2011) 1305.
[11] T. Yatsuhashi, N. Nakashima, J. Phys. Chem. A 109 (2005).
[12] M. Murakami, R. Mizoguchi, Y. Shimada, T. Yatsuhashi, N. Nakashima, Chem. Phys. Lett. 403 (2005) 238.
[13] M. Tanaka, M. Kawaji, T. Yatsuhashi, N. Nakashima, J. Phys. Chem. A 113 (2009) 12056.
[14] T. Bohinski, K. Moore, K. Moore Tibbetts, M. Tarazkar, D. Romanov, S. Matsika, R.J. Levis, J. Phys. Chem. Lett. 4 (2013) 1587.
[15] T. Bohinski, K. Moore Tibbetts, M. Tarazkar, D.A. Romanov, S. Matsika, R.J. Levis, (submitted for publication).
[16] S.A. Trushin, W. Fuss, W.E. Schmid, Physics 37 (2004) 3987.
[17] D. Wu, Q.Q. Wang, X.H. Cheng, M.X. Jin, X.Y. Li, Z. Hu, D. Ding, J. Phys. Chem. A 111 (2007) 9494.
[18] T. Yatsuhashi, N. Nakashima, J. Phys. Chem. A 114 (2010) 7445.
[19] J.W. Ho, W.K. Chen, P.Y. Cheng, J. Chem. Phys. 131 (2009).
[20] C. Trallero, B.J. Pearson, T. Weinacht, K. Gilliard, S. Matsika, J. Chem. Phys. 128 (2008).
[21] S. Amarie, K. Arefe, J.H. Starcke, A. Dreuw, J. Wachtveitl, J. Phys. Chem. B 112 (2008) 14011.
[22] C. Zhou, S. Matsika, M. Kotur, T.C. Weinacht, J. Phys. Chem. A 116 (2012) 9217.
[23] B.J. Pearson, S.R. Nichols, T. Weinacht, J. Chem. Phys. 127 (2007).
[24] J. Gonzalez-Vazquez, L. Gonzalez, S.R. Nichols, T.C. Weinacht, T. Rozgonyi, PCCP 12 (2010) 14203.
[25] S.M. Hankin, D.M. Villeneuve, P.B. Corkum, D.M. Rayner, Phys. Rev. A: At. Mol. Opt. Phys. 64 (2001).
[26] M.J. Frisch, G.W. Trucks, H.B. Schlegel, G.E. Scuseria, M.A. Robb, J.R. Cheeseman, G. Scalmani, V. Barone, B. Mennucci, G.A. Petersson, H. Nakatsuji, M. Caricato, X. Li, H.P. Hratchian, A.F. Izmaylov, J. Bloino, G. Zheng, J.L. Sonnenberg, M. Hada, M. Ehara, K. Toyota, R. Fukuda, J. Hasegawa, M. Ishida, T. Nakajima, Y. Honda, O. Kitao, H. Nakai, T. Vreven, J.A. Montgomery, J.E. Peralta, F. Ogliaro, M. Bearpark, J.J. Heyd, E. Brothers, K.N. Kudin, V.N. Staroverov, R. Kobayashi, J. Normand, K. Raghavachari, A. Rendell, J.C. Burant, S.S. Iyengar, J. Tomasi, M. Cossi, N. Rega, J.M. Millam, M. Klene, J.E. Knox, J.B. Cross, V. Bakken, C. Adamo, J. Jaramillo, R. Gomperts, R.E. Stratmann, O. Yazyev, A.J. Austin, R. Cammi, C. Pomelli, J.W. Ochterski, R.L. Martin, K. Morokuma, V.G. Zakrzewski, G.A. Voth, P. Salvador, J.J. Dannenberg, S. Dapprich, A.D. Daniels, Farkas, J.B. Foresman, J.V. Ortiz, J. Cioslowski, D.J. Fox, Gaussian 09, Revision B.01, Inc., Wallingford CT, 2009.
[27] T. Giroldo, J.M. Riveros, J. Phys. Chem. A 106 (2002) 9930.
[28] T. Kobayashi, S. Nagakura, Bull. Chem. Soc. Jpn. 47 (1974) 2563.